Real and complex Li-Sinai solutions of the 3D incompressible Navier-Stokes equations

Carlo Boldrighini, Sandro Frigio, Pierluigi Maponi, Alessandro Pellegrinotti, and Yakov G. Sinai

Abstract. In the framework of the Global Regularity Problem for the incompressible Navier-Stokes (NS) equations in the whole space $\mathbb{R}^3$, Li and Sinai in [*J. Eur. Math. Soc.*, 10:267–313, 2008] proved the existence of smooth complex solutions that become singular ("blow-up") in a finite time. We report new results obtained by computer simulations on the behavior of complex solutions with support of Li-Sinai type and of real flows related to them. For the complex solutions the simulations indicate that the class of initial data leading to a blow-up is much larger than that considered by Li and Sinai. The real flows show some remarkable properties, such as a sharp increase of the total enstrophy and a concentration of high values of velocities and vorticity in small regions. We conclude with a discussion on the perspectives of a real blow-up in the framework of the Li-Sinai approach.

Keywords. Incompressible Navier-Stokes, singular solutions, blow-up, tornadoes.

1   Introduction

The Global Regularity Problem (GRP) for the incompressible Navier-Stokes equations in $\mathbb{R}^3$, i.e., whether there are smooth solutions that become singular in a finite time, is still open (see, e.g., [19]), although it dates back to the pioneering work of J. Leray [12] in 1934, and in spite of the extensive literature devoted to it. In recent times, results of discrete dyadic models of the Euler and NS equations which preserve the energy conservation, introduced by Katz and Pavlovic in [6], [10], seem to indicate that there are singular solutions at finite times (blow-up). Also, T. Tao [18] proved a blow-up for a continuous NS model obtained by modifying the bilinear term in such a way that the energy conservation is preserved.

The existence of singularities is not just a fact of theoretical importance. We know that if the solution becomes singular the total enstrophy diverges in an integrable way (in time) and the solution becomes infinite at some points [17], and clearly the solutions near the blow-up time would provide a description of a new type of "extreme" phenomena occurring in fluid motion.

In a paper appeared in 2008 [13], Li and Sinai proposed a new approach to the problem, consisting in the explicit construction of singular solutions. They write the 3D NS equations as an integral equation in Fourier **k**-space and consider a class of initial data with essential support in a sphere of radius r at some distance from the origin, centered around some point $\mathbf{k}_0$ with $|\mathbf{k}_0| > r$. By the convolution mechanism, due to the nonlinear term, the support of the solution undergoes a rapid extension to the region of high $|\mathbf{k}|$ values, along the direction $\mathbf{k}_0$, with a corresponding increase of the total enstrophy. The solution can then be represented by a series of p-fold convolutions $\mathbf{g}^{(p)}$ with support in a region around the point $p\mathbf{k}_0$, and the authors show that as $p \to \infty$ there are fixed points of a suitable renormalization map $\mathbf{g}^{(p)} \to \mathbf{g}^{(p+1)}$, identified as solutions of a fixed point equation. They choose a particularly simple fixed point and construct a set of initial data for which the asymptotics of the renormalized functions $\mathbf{g}^{(p)}$ leads to the chosen fixed point and to a finite-time blow-up. The proofs are based on Renormalization Group Techniques and are rather lengthy and involved.

The results of the paper [13] are important, but they are not a solution of the GRP, because solutions with support in **k**-space as described above correspond to complex solutions in the physical **x**-space. They are also unphysical, in that the total energy diverges together with the total enstrophy.

The simplest way to obtain real (physical) solutions which share with the complex solutions a rapid extension of the support in the direction of the high $|\mathbf{k}|$ region, is that of antisymmetrizing the initial data of Li and

Sinai. That is, we take initial data of the type $\mathbf{v}_0(\mathbf{k}) - \mathbf{v}_0(-\mathbf{k})$, where $\mathbf{v}_0$ are data leading to a blow up in the complex case, so that the initial data for the real flow are supported in two symmetric regions around the points $\pm\mathbf{k}_0$. As in the one-sided (complex) case, the convolutions extend the support in the directions $\pm\mathbf{k}_0$, but there is a damping interference of the terms coming from the two supports.

The theoretical difficulties of the real case are harder than in the complex case and really daunting. It is natural in such cases to resort to computer simulations for a better understanding of the behavior of the solutions, and for a guideline of theoretical research. And indeed computer simulations for the Global Regularity Problem were done in the past (see, e.g., [9]), but the evidence is inconclusive.

In fact, a theoretical guide-line is needed in order to control the difficulties arising in computing solutions of the three-dimensional Navier-Stokes equations for high values of the velocity and the vorticity. In our case it is of great help that the support of the solution in Fourier space is concentrated along an axis, which makes the computer simulations much easier.

We first performed computer simulations for the complex case considered by Li and Sinai [3], with the help of a new computer program for simulations of the NS equations represented as an integral equation in Fourier space. The results showed that for a rather wide range of the parameters it is possible to follow the solutions up to times very close to the blow-up. It was also possible to obtain good estimates of the critical time τ, thanks to the fact that, as predicted by the Li-Sinai theory, the log of the marginal distribution of the energy along the axis $\mathbf{k}_0$ behaves linearly with a slope proportional to $\tau - t$.

In the past few years we also performed simulations for the real case obtained by antisymmetrizing the initial data of the case in [13]. The results [4], [5] show that in some range of the parameters the solutions behave initially as the complex ones, showing a rapid increase of the total enstrophy and of the maximal velocity, with concentration of the energy in a small region. Then, after some time there is a relaxation with decrease of the total energy. It should be noted that for such solutions a blow-up is not expected, as they are axial symmetric, with no swirl, or close to that (see [11]).

In this paper we present results from recent computer simulations performed at the TGCC Joliot Curie, partition irene-knl, within the framework of the European PRACE Project 2021240097.

We performed simulations both for complex solutions and for real ones. For the complex solutions the aim was to understand whether initial data related to the solutions of the Li-Sinai fixed point equations are necessary for a blow-up. The results indicate that the blow-up for complex solutions

with initial support in **k** space as described above is a much more general phenomenon.

We also show results of simulations for real flows with initial support in Fourier space concentrated in relative small regions around some points $\pm\mathbf{k}_0$, as described above, but otherwise unrelated to the Li-Sinai fixed points. For a particular such solution, which is axial symmetric with nonzero swirl, we found that the initial enstrophy increases by a factor about 20, 10 times more than for the case in [4], [5]. We also report other interesting features of the simulations.

The problem whether real solutions with support in **k**-space extending along an axis can exhibit a finite-time blow-up remains open. We did not have enough computer time to study simulations for cases with an expansion along two different axes, which could also be feasible with the present-day supercomputers.

The plan of our paper is as follows. In §2 we sketch the outline of the results of Li and Sinai, then in §3 we report recent results of the blow-up of complex solutions unrelated to the fixed point solutions, and finally §4 is devoted to the discussion of results for real flows of the Li-Sinai type.

2   The Li-Sinai approach

We consider the NS equations in the whole space $\mathbb{R}^3$

$$\frac{\partial \mathbf{u}}{\partial t} + \sum_{j=1}^{3} u_j \frac{\partial}{\partial x_j} \mathbf{u} = \Delta \mathbf{u} - \nabla p, \qquad \mathbf{x} = (x_1, x_2, x_3) \in \mathbb{R}^3. \qquad (2.1)$$

$$\nabla \cdot \mathbf{u} = \sum_{j} \frac{\partial}{\partial x_j} u_j = 0, \qquad \mathbf{u}(\cdot, 0) = \mathbf{u}_0. \qquad (2.2)$$

The value of the viscosity is $\nu = 1$, which is not restrictive, as it can always be obtained by rescaling. The pressure p ensures incompressibility and is obtained in terms of the velocity field **u** by solving the Poisson equation

$$\nabla \cdot \sum_{j=1}^{3} u_j \frac{\partial}{\partial x_j} \mathbf{u} = -\Delta \mathbf{p}. \qquad (2.3)$$

In the formulation of Li and Sinai we consider the modified Fourier transform

$$\mathbf{v}(\mathbf{k}, t) = \frac{i}{(2\pi)^3} \int_{\mathbb{R}^3} \mathbf{u}(\mathbf{x}, t) e^{-i\langle \mathbf{k}, \mathbf{x} \rangle} d\mathbf{x}, \qquad \mathbf{k} = (k_1, k_2, k_3) \in \mathbb{R}^3, \quad (2.4)$$

where $\langle \cdot, \cdot \rangle$ denotes the scalar product. Taking into account the solenoidality condition $\langle \mathbf{k}, \mathbf{v}(\mathbf{k}, t) \rangle = 0$, the equation for $\mathbf{v}(\mathbf{k}, t)$ takes the form

$$\frac{\partial \mathbf{v}(\mathbf{k}, \mathbf{t})}{\partial t} + \mathbf{k}^2 \mathbf{v}(\mathbf{k}, t) = \int_{\mathbb{R}^3} \langle \mathbf{v}(\mathbf{k} - \mathbf{k}', t), \mathbf{k} \rangle P_{\mathbf{k}} \mathbf{v}(\mathbf{k}', t) d\mathbf{k}' \qquad (2.5)$$

where $P_{\mathbf{k}} \mathbf{v} = \mathbf{v} - \frac{\langle \mathbf{v}, \mathbf{k} \rangle}{\mathbf{k}^2} \mathbf{k}$ is the projection orthogonal to $\mathbf{k}$, and the initial condition is $\mathbf{v}(\mathbf{k}, 0) = \mathbf{v}_0(\mathbf{k})$, and $\mathbf{v}_0$ is the transform of $\mathbf{u}_0$.

Li and Sinai assume that $\mathbf{v}$ is a real function, which, by the inverse formula

$$\mathbf{u}(\mathbf{x}, t) = -i \int_{\mathbb{R}^3} e^{i\langle \mathbf{k}, \mathbf{x} \rangle} \mathbf{v}(\mathbf{k}, t) d\mathbf{k}, \qquad (2.6)$$

implies that $\mathbf{u}(\mathbf{x}, t)$ is in general a complex function, and describes a real flow only if $\mathbf{v}(\mathbf{k}, t)$ is antisymmetric in $\mathbf{k}$, which implies that $\mathbf{u}(\mathbf{x}, t)$ is also antisymmetric in $\mathbf{x}$.

By a Duhamel formula the incompressible Navier-Stokes equations take the form of a single integral equation

$$\mathbf{v}(\mathbf{k}, t) = e^{-t\mathbf{k}^2} \mathbf{v}_0(\mathbf{k}) + \int_0^t e^{-(t-s)|\mathbf{k}|^2} \int_{\mathbb{R}^3} \langle \mathbf{v}(k - k', s), \mathbf{k} \rangle P_{\mathbf{k}} \mathbf{v}(\mathbf{k}', s) d\mathbf{k}' ds. \qquad (2.7)$$

For the analysis that follows it is convenient to multiply the initial data by a real number A, so that, iterating the Duhamel formula, the solution of the equation (2.5) is represented as a power series

$$\mathbf{v}(\mathbf{k}, t) = A\mathbf{g}^{(1)}(\mathbf{k}, t) + \sum_{p=2}^{\infty} A^p \int_0^t e^{-\mathbf{k}^2(t-s)} \mathbf{g}^{(p)}(\mathbf{k}, s) ds, \qquad (2.8)$$

where $\mathbf{g}^{(1)}(\mathbf{k}, s) = e^{-s\mathbf{k}^2} \mathbf{v}_0(\mathbf{k})$, and the following terms are convolutions:

$$\mathbf{g}^{(2)}(\mathbf{k}, s) = \int_{\mathbb{R}^3} \left\langle \mathbf{g}^{(1)}(\mathbf{k} - \mathbf{k}', s), \mathbf{k} \right\rangle P_{\mathbf{k}} \mathbf{g}^{(1)}(\mathbf{k}', s) d\mathbf{k}', \qquad (2.9)$$

$$\mathbf{g}^{(p)}(\mathbf{k}, s) =$$

$$= \int_0^s ds_2 \int_{\mathbb{R}^3} \langle \mathbf{v}_0(\mathbf{k} - \mathbf{k}'), \mathbf{k} \rangle P_{\mathbf{k}} \mathbf{g}^{(p-1)}(\mathbf{k}', s_2) e^{-s(\mathbf{k} - \mathbf{k}')^2 - (s - s_2)(\mathbf{k}')^2} d\mathbf{k}' +$$

$$+ \sum_{\substack{p_1 + p_2 = p \\ p_1, p_2 > 1}} \int_0^s ds_1 \int_0^s ds_2 \int_{\mathbb{R}^3} \left\langle \mathbf{g}^{(p_1)}(\mathbf{k} - \mathbf{k}', s_1), \mathbf{k} \right\rangle \cdot$$

$$\cdot P_{\mathbf{k}}\mathbf{g}^{(p_2)}(\mathbf{k}', s_2)e^{-(s-s_1)(\mathbf{k}-\mathbf{k}')^2-(s-s_2)(\mathbf{k}')^2}d\mathbf{k}'+ \qquad (2.10)$$

$$+\int_0^s ds_1 \int_{\mathbb{R}^3} \left\langle \mathbf{g}^{(p-1)}(\mathbf{k}-\mathbf{k}', s_1), \mathbf{k} \right\rangle P_{\mathbf{k}}\mathbf{v}_0(\mathbf{k}')e^{-(s-s_1)(\mathbf{k}-\mathbf{k}')^2-s(\mathbf{k}')^2}d\mathbf{k}'.$$

Proposition 2.1. *If* $\mathbf{v}_0 \in L_\infty(\mathbb{R}^3) \cap L_1(\mathbb{R}^3)$ *the series (2.8) converges absolutely if* $|At^{\frac{1}{2}}|$ *is small enough.*

Proof. Let $\phi_0(\mathbf{k}) = |\mathbf{v}^{(0)}(\mathbf{k})|$. Then if $p \geq 2$ the following inequality holds

$$\left|\mathbf{g}^{(p)}(\mathbf{k}, s)\right| \leq K^{p-1} \sqrt{p} s^{\frac{p-3}{2}} \phi_0^{(p)}(\mathbf{k}), \qquad (2.11)$$

where K is a positive constant and $\phi_0^{(p)}(\mathbf{k}) = (\phi_0 * \ldots * \phi_0)(\mathbf{k})$ is a repeated convolution.

In fact, clearly $|\mathbf{g}^{(1)}(\mathbf{k})| \leq \phi_0(\mathbf{k})$. As for $\mathbf{g}^{(2)}$, we can replace $\mathbf{k}$ by $\mathbf{k}'$ in the scalar product (2.9), by solenoidality, so that

$$\left|\mathbf{g}^{(2)}(\mathbf{k}, s)\right| \leq \int_{\mathbb{R}^3} \phi_0(\mathbf{k}-\mathbf{k}')|\mathbf{k}'|e^{-s|\mathbf{k}'|^2}\phi_0(\mathbf{k}')d\mathbf{k} \leq \frac{c_1}{\sqrt{s}}\phi_0^{(2)}(\mathbf{k}), \quad (2.12)$$

where $c_1 =: \max |x|e^{-x^2} = (2e)^{-\frac{1}{2}}$. For $p > 2$ we proceed by induction. We write (2.10) as

$$\mathbf{g}^{(p)}(\mathbf{k}, s) = \sum_{p_1+p_2=p} \mathbf{g}^{(p_1,p_2)}(\mathbf{k}, s),$$

$$\mathbf{g}^{(p_1,p_2)}(\mathbf{k}, s) = \int_0^s ds_1 \int_0^s ds_2 \mathbf{g}^{(p_1,p_2)}(s; s_1, s_2), \qquad (2.13)$$

$$\mathbf{g}^{(p_1,p_2)}(s; s_1, s_2) =$$

$$= \int_{\mathbb{R}^3} \left\langle \mathbf{g}^{(p_1)}(\mathbf{k}-\mathbf{k}', s_1), \mathbf{k} \right\rangle P_{\mathbf{k}}\mathbf{g}^{(p_2)}(\mathbf{k}', s_2)e^{-(s-s_1)(\mathbf{k}-\mathbf{k}')^2-(s-s_2)(\mathbf{k}')^2}d\mathbf{k}',$$

and consider the case $p_1, p_2 > 1$. Again replacing $\mathbf{k}$ by $\mathbf{k}'$ and proceeding as before, we get by the Ansatz (2.11)

$$\int_0^s ds_1 \int_0^s ds_2 \left|\mathbf{g}^{(p_1,p_2)}(s; s_1, s_2)\right| \leq$$

$$\leq c_1 \int_0^s ds_1 \int_0^s \frac{ds_2}{\sqrt{s-s_2}} \int_{\mathbb{R}^3} |\mathbf{g}^{(p_1)}(\mathbf{k}-\mathbf{k}', s_1)||\mathbf{g}^{(p_2)}(\mathbf{k}', s_2)|d\mathbf{k}' \leq$$

$$\leq c_1 K^{p-2} \sqrt{p_1 p_2} \int_0^s s_1^{\frac{p_1-3}{2}} ds_1 \int_0^s \frac{s_2^{\frac{p_2-3}{2}}}{\sqrt{s-s_2}}ds_2 \, \phi_0^{(p)}(\mathbf{k}). \qquad (2.14)$$

Integrating in s_1 and setting in the second integral $s_2 = su$ the coefficient of $\phi_0^{(p)}$ is

$$\frac{2c_1}{p_1 - 1}\sqrt{p_1 p_2} K^{p-2} s^{\frac{p-3}{2}} \int_0^1 \frac{u^{\frac{p_2-3}{2}}}{\sqrt{1-u}} du. \qquad (2.15)$$

The change of variable $u = \sin^2 \theta$ gives

$$\int_0^1 \frac{u^{\frac{p_2-3}{2}}}{\sqrt{1-u}} du = 2 \int_0^{\frac{\pi}{2}} (\sin \theta)^{p_2-2} d\theta =: 2J_{p_2-2}.$$

We see that $J_0 = \frac{\pi}{2}$, $J_1 = 1$ and the recurrence relation $J_{n+1} = \frac{n}{n+1} J_{n-1}$ holds, so that

$$J_{2n} = \frac{(2n-1)!!}{(2n)!!}\frac{\pi}{2}, \qquad J_{2n+1} = \frac{(2n)!!}{(2n+1)!!}. \qquad (2.16)$$

As $J_{2n}J_{2n+1} = \frac{\pi}{2(2n+1)}$ we have $J_p \leq \frac{c_2}{\sqrt{p+1}}$, $c_2 > 0$. Hence the quantity (2.15) is smaller than

$$s^{\frac{p-3}{2}} \frac{4c_1 c_2\ K^{p-2}}{(p_1-1)\sqrt{p_2-1}}\sqrt{p_1 p_2}.$$

Moreover there is a constant $c_3 > 0$ such that

$$\sum_{\substack{p_1+p_2=p \\ p_1,p_2>1}} \frac{\sqrt{p_1 p_2}}{(p_1-1)\sqrt{p_2-1}} \leq c_3\sqrt{p}.$$

It is easy to see that the boundary terms $(p_1, p_2) = (1, p-1)$ and $(p_1, p_2) = (p-1, 1)$ give a contribution which is bounded in absolute value by $c_4 K^{p-2}\phi_0^{(p)}(\mathbf{k})$.

Hence (2.11) is proved for any $K > 4c_1 c_2 c_3 + c_4$.

If now $\mathbf{v}_0 \in L_\infty \cap L_1$ we have $\phi_0(\mathbf{k}) = N\widehat{\phi}_0(\mathbf{k})$ where $N = \int_{\mathbb{R}^3} \phi_0(\mathbf{k})d\mathbf{k}$ and $\widehat{\phi}_0(\mathbf{k})$ is a probability density on $\mathbb{R}^3$. Hence the convolution is $\widehat{\phi}_0^{(p)}(\mathbf{k}) = N^{-p}\phi_0^{(p)}(\mathbf{k})$ is also a probability density. Therefore

$$\phi_0^{(p)}(\mathbf{k}) \leq N^p \|\widehat{\phi}_0\|_\infty \|\widehat{\phi}^{(p-1)}\|_1 = N^p \|\widehat{\phi}_0\|_\infty.$$

The proposition is proved. $\qquad\qquad\qquad\qquad\qquad\qquad\qquad\qquad\qquad \square$

We choose initial data with support $C = \operatorname{supp} \mathbf{v}_0$, in a sphere of center $\mathbf{k}_0$ of radius $R << |\mathbf{k}_0|$. It is not restrictive to take $\mathbf{k}_0 = (0, 0, a)$, $a > 0$, so that by iteration of the convolution, the support $\underbrace{C + \ldots + C}_{p\ times}$ of $\mathbf{g}^{(p)}$ extends along the k_3-axis around $p\mathbf{k}^{(0)}$. By analogy with probability theory,

for large p the main contribution to $\mathbf{g}^{(p)}$ is concentrated in a region with transversal dimensions of the order $\sqrt{p}$.

Moreover for large p the terms of the sum for which $\max\{p_1, p_2\} \le p^{\frac{1}{2}}$ can be neglected, and the Gaussian densities give a significant contribution to the integrals only for s_1, s_2 near the endpoint s. Therefore it is natural to introduce new variables and functions

$$\mathbf{k} = p\mathbf{k}^{(0)} + \sqrt{p}\mathbf{Y}, \qquad \mathbf{h}^{(p)}(\mathbf{Y}, s) = \mathbf{g}^{(p)}(p\mathbf{k}^{(0)} + \sqrt{p}\mathbf{Y}, s),$$

$$s_j = s\left(1 - \frac{\theta_j}{p_j^2}\right), \qquad j = 1, 2.$$

Integrating over $\theta_j, j = 1, 2$, setting $\gamma = \frac{p_1}{p}$ and $\mathbf{e}_3 = (0, 0, 1)$, we get

$$\mathbf{h}^{(p)}(\mathbf{Y}, s) = p^{\frac{5}{2}} \sum_{\substack{p_1 + p_2 = p \\ p_1, p_2 > \sqrt{p}}} \frac{1}{p_1^2 p_2^2} \int_{\mathbb{R}^3} P_{\mathbf{e}_3 + \frac{\mathbf{Y}}{\sqrt{p}}} \mathbf{h}^{(p_2)}\left(\frac{\mathbf{Y}'}{\sqrt{1-\gamma}}, s\right) \cdot \qquad (2.17)$$

$$\cdot \left\langle \mathbf{h}^{(p_1)}\left(\frac{\mathbf{Y} - \mathbf{Y}'}{\sqrt{\gamma}}, s\right), \mathbf{e}_3 + \frac{\mathbf{Y}}{\sqrt{p}} \right\rangle d\mathbf{Y}' \ (1 + o(1)),$$

As $\mathbf{h}^{(p)}$ is orthogonal to $\mathbf{k} = (\sqrt{p}Y_1, \sqrt{p}Y_2, pa + \sqrt{p}Y_3)$, by incompressibility, we also set

$$\mathbf{h}^{(p)}(\mathbf{Y}, s) = \left(H_1^{(p)}(\mathbf{Y}, s), H_2^{(p)}(\mathbf{Y}, s), \frac{F^{(p)}(\mathbf{Y}, s)}{\sqrt{p}\, a}\right), \qquad (2.18)$$

and $F^{(p)}(\mathbf{Y}, s)$ is of finite order:

$$Y_1 H_1^{(p)}(\mathbf{Y}, s) + Y_2 H_2^{(p)}(\mathbf{Y}, s) + F^{(p)}(\mathbf{Y}, s) = \mathcal{O}(p^{-\frac{1}{2}} a^{-1}). \qquad (2.19)$$

Therefore $\mathbf{h}^{(p)}(\mathbf{Y}, s)$ is essentially transversal to the k_3-axis, and as $p \to \infty$, $P_{\mathbf{e}_3 + \frac{\mathbf{Y}}{\sqrt{p}}} \mathbf{h}^{(p_2)} \to \mathbf{h}^{(p_2)}$, i.e., the solenoidal projector in (2.17) tends to the identity.

The fundamental *Ansatz* of Li and Sinai is that for some set of initial data $\mathbf{v}_0$, for p large and s in some interval of time, the recursive relation (2.17) has a solution which is asymptotically of the form

$$\mathbf{h}^{(p)}(\mathbf{Y}, s) = Z\, p\, \Lambda_p(s) \prod_{j=1}^{3} g_{\sigma_j}(Y_j) \left(\mathbf{H}(\mathbf{Y}) + \delta^{(p)}(\mathbf{Y}, s)\right), \qquad (2.20)$$

where $\delta^{(p)}(\mathbf{Y}, s) \to 0$ as $p \to \infty$. Here Z is a suitable constant, $\Lambda_p(s)$ is a positive function, $g_\sigma(x) = \frac{e^{-\frac{x^2}{2\sigma}}}{\sqrt{2\pi\sigma}}$ denotes the centered Gaussian density

on $\mathbb{R}$, $\sigma_1, \sigma_2, \sigma_3$ are positive constants, $\mathbf{H} = (H_1(\mathbf{Y}), H_2(\mathbf{Y}), 0)$ is a vector function independent of time depending only on Y_1, Y_2. By rescaling it is not restrictive to set $\sigma_i = 1$, $i = 1, 2, 3$.

Inserting (2.20) into (2.17), treating γ as a continuous variable, neglecting the remainders, choosing the constant Z in a suitable way, and integrating over Y_3, one can see that $\mathbf{H}(\mathbf{Y})$ is a solution of the integral fixed point equation

$$g_1(\mathbf{Y})\mathbf{H}(\mathbf{Y}) = \int_0^1 d\gamma \int_{\mathbb{R}^2} g_\gamma(\mathbf{Y} - \mathbf{Y}')g_{1-\gamma}(\mathbf{Y}') \cdot$$

$$\cdot \mathcal{L}(\mathbf{H}; \gamma, \mathbf{Y}, \mathbf{Y}')\mathbf{H}\left(\frac{\mathbf{Y}'}{\sqrt{1-\gamma}}\right) d\mathbf{Y}'$$

(2.21)

where, by abuse of notation, we write $\mathbf{Y} = (Y_1, Y_2)$, $g_\sigma(\mathbf{Y}) = \frac{e^{-\frac{Y_1^2 + Y_2^2}{2\sigma}}}{2\pi\sigma}$, and set

$$\mathcal{L}(\mathbf{H}; \gamma, \mathbf{Y}, \mathbf{Y}') = (1-\gamma)^{\frac{3}{2}} \left\langle \frac{\mathbf{Y} - \mathbf{Y}'}{\sqrt{\gamma}}, \mathbf{H}\left(\frac{\mathbf{Y} - \mathbf{Y}'}{\sqrt{\gamma}}\right)\right\rangle +$$

$$+ \gamma^{\frac{1}{2}}(1-\gamma) \left\langle \frac{\mathbf{Y}'}{\sqrt{1-\gamma}}, \mathbf{H}\left(\frac{\mathbf{Y}'}{\sqrt{1-\gamma}}\right)\right\rangle.$$

The solutions, or "fixed points", of the functional equation (2.21) are found by expanding the components of $\mathbf{H}$ in Hermite polynomials He_k, $k = 0, 1, \ldots$.

$$H_j(\mathbf{Y}) = \sum_{m_1, m_2=0}^{\infty} h_{m_1 m_2}^{(j)} \mathrm{He}_{m_1}(Y_1)\,\mathrm{He}_{m_2}(Y_2), \qquad j = 1, 2. \qquad (2.22)$$

One gets an infinite system of equations for the components $h_{m,n}^{(j)}$, which has infinitely many solutions depending on a small number of arbitrary parameters (see [13]). For one particularly simple solution, namely $h_{1,0}^{(1)} = h_{0,1}^{(2)} = -2$ and $h_{n,m}^{(j)} = 0$ otherwise, corresponding to the fixed point

$$\mathbf{H}(k_1, k_2) = \mathbf{H}_0(k_1, k_2) := -2\,(k_1, k_2)\,, \qquad (2.23)$$

Li and Sinai prove in [13] the following result:

Theorem 2.2. *For the fixed point (2.23) one can find an interval $S = [s_-, s_+]$, $s_+ > s_-$, and a 10-parameter family of initial conditions such that for $s \in S$ the Ansatz (2.20) holds with $\Lambda_p(s) = (\Lambda(s))^p$ where $\Lambda(s)$ is a strictly increasing differentiable function with $\min_{s \in S} \Lambda'(s) \geq B > 0$, and*

$$\sup_Y |\delta^{(p)}(Y, s)| \to 0 \ as \ p \to \infty.$$

The proof is based on a renormalization group method, with a rather involved linearized stability analysis around the fixed point.

If now the initial data are chosen as stated in the above theorem, then the asymptotics (2.20) holds for $\mathbf{H} = \mathbf{H}_0$ and if we set $A = \pm(\Lambda(\tau))^{-1}$, for $\tau \in S$, in the expansion (2.8), there is a blow-up at the time $t = \tau$. As shown in the paper [5], if there are cancellations between terms of the series (2.8) with neighboring p, which for the fixed point $\mathbf{H}_0$ holds for positive A, the total enstrophy diverges at the blow-up time as $\mathrm{const}(\tau - t)^{-\frac{5}{2}}$, and for negative A as $\mathrm{const}(\tau - t)^{-3}$. Another easy result shown in [3], [5], is that the solution $\mathbf{v}(\mathbf{k}, t)$ tends pointwise to a finite limit as $t \uparrow \tau$.

3   Computer simulations for the complex blow-up with and without fixed points

Our mesh for the computer simulations of the solution of equation (2.7) is always a regular lattice centered at the origin with step $\delta = 1$, i.e., a subset of the unitary lattice $\mathbb{Z}^3$ in $\mathbf{k}$-space, with maximal configuration $[-L_1, L_1] \times [-L_1, L_1] \times [-9, L]$, where L_1 is of the order of the hundreds and L of the order of the thousands. The velocity field $\mathbf{v}(\mathbf{k}, t)$ is therefore represented by an array of about $3 \times L_1^2 \times L$ real numbers, close to the maximal capacity of modern supercomputers. The flow in $\mathbf{x}$-space is confined to a small region inside the cube $(-\pi, \pi)^3$.

The mesh with step $\delta = 1$, is reliable for our choice of the initial data: we checked that by taking a smaller δ there is no significant change in the behavior of the total energy, the total enstrophy and their marginal distributions.

As we mentioned above, the real solutions associated to the Li-Sinai complex solution with fixed point (2.23) are close to axial symmetric with zero swirl, and a blow-up is therefore excluded [11]. It is natural to look for other complex solutions that blow up and are such that the associated real solutions have a significant swirl.

We looked for indications from computer simulations for solutions related to solutions of the fixed point equation (2.21) different from (2.23), among which there are flows that are not axial symmetric, as well as axial symmetric flows with swirl. We also simulated solutions with initial data concentrated in a small region at some distance from the origin, as explained above, but unrelated to fixed points.

We need a brief discussion on some solutions of the fixed point equation that are not reported in [13]. As shown in that paper, the fixed point equation for the coefficients of the expansion in Hermite polynomials (2.22)

has the form

$$
h_{m,n}^{(j)} = \sum_{\substack{m_1+n_1=m \\ m_2+n_2=n}} \sum_{\ell=1}^{2} \Big(J_{m_1+m_2,n_1+n_2}^{(1)} (B_\ell h^{(\ell)})_{m_1,m_2} h_{n_1,n_2}^{(j)} +
$$

$$
+ \, J_{m_1+m_2,n_1+n_2}^{(2)} h_{m_1,m_2}^{(\ell)} (B_\ell h^{(j)})_{n_1,n_2} \Big). \quad (3.1)
$$

where we assume $h_{0,0}^{(j)} = 0$, $j = 1, 2$ and we set

$$
(B_1 h^{(j)})_{m,n} = h_{m-1,n}^{(j)} + (m+1) h_{m+1,n}^{(j)},
$$

$$
(B_2 h^{(j)})_{m,n} = h_{m,n-1}^{(j)} + (n+1) h_{m,n+1}^{(j)}, \quad j = 1, 2., \quad (3.2)
$$

The coefficients are

$$
J_{m,n}^{(1)} = -I_{m,n+3}, \qquad J_{m,n}^{(2)} = I_{m+1,n+2},
$$

$$
I_{m,n} = \int_0^1 \gamma^{\frac{m}{2}} (1-\gamma)^{\frac{n}{2}} d\gamma = \frac{\Gamma(\frac{m}{2}+1)\Gamma(\frac{n}{2}+1)}{\Gamma(\frac{m+n}{2}+2)}, \quad (3.3)
$$

where Γ is the Euler Gamma function.

The equation (3.1) has the following structure. The equations for $m + n \le N$, for $N = 1, 2, \ldots$ are closed so that the equation can be solved by an iteration method, i.e., the equations for $\{h_{n,m}^{(j)} : n+m = N\}$, $N = 2, \ldots$ are a set of $2N+2$ linear equations with coefficients and known terms given by the solutions of the equations for $\{h_{n,m}^{(j)} : n + m = M\}$ with $M < N$.

For $N = 1$ we have a nonlinear homogeneous system for the variables $\{h_{1,0}^{(1)}, h_{0,1}^{(1)}, h_{1,0}^{(2)}, h_{0,1}^{(2)}\}$. In addition to the trivial solution, we have a family of two-parameter solutions, which, taking as parameters $h_{0,1}^{(1)} = w, h_{1,0}^{(2)} = y$, are real for $wy \le 9$ and can be written as

$$
\left(-3 \pm \sqrt{9 - wy}, \; w, \; y, \; -3 \mp \sqrt{9 - wy} \right). \quad (3.4)
$$

There is also an additional separate solution $(-2, 0, 0, -2)$.

For any choice of the solution for $N = 1$, the linear set of equations for $N = 2$ is homogeneous with nonzero determinant, so that there is only the trivial solution. The same happens for all sets of equations with N even, so that $h_{m,n}^{(j)} = 0$, $j = 1, 2$, whenever $m + n$ is even.

For $N = 3$ the system is also homogeneous, but has nontrivial solutions, depending on the solutions for $N = 1$. By taking the trivial solutions for $N = 3$ all the following orders are homogeneous, so that the solutions for $N = 1$ are full solutions of the fixed point equation. In particular the separate solution $(-2, 0, 0, -2)$ corresponds to the choice (2.23) in [13].

A more detailed discussion shows that the equations for $N = 3$ have a 3-parameter family of nontrivial solutions if we take the solution (2.23) for $N = 1$, and in general a 4-parameter one if we take one of the solutions (3.4). In [13] it is shown that taking the solution (2.23) for $N = 1$, and the parameters of the nontrivial solution for $N = 3$ small enough, the infinite series of the full solution that follows converges absolutely.

We performed computer simulations for initial data corresponding to one solution of the fixed point equations of the type (3.4), and also for initial data unrelated to fixed points. We always choose the center of the support on the positive k_3-axis, i.e., we take $\mathbf{k}_0 = (0, 0, a)$, $a > 0$. Following the indications of [13], the initial data corresponding to a fixed point $\mathbf{H}$ are taken of the following type

$$\left(\tilde{H}_1(k_1, k_2), \tilde{H}_2(k_1, k_2), -\frac{k_1 \tilde{H}_1(k_1, k_2) + k_2 \tilde{H}_2(k_1, k_2)}{k_3} \right).$$

$$\cdot g_\sigma(k_1) g_\sigma(k_2) g_\sigma(k_3 - a) \chi_\eta(k_3 - a), \quad (3.5)$$

where $0 < \sigma < \eta < a$ and $\chi_\eta(x) = 1$ for $|x| < \eta$ and $\chi_\eta(x) = 0$ otherwise. Moreover $\tilde{H}_j(k_1, k_2) = H_j(k_1, k_2) + \delta_j(k_1, k_2)$, with $\delta_j(k_1, k_2)$, $j = 1, 2$, are small perturbations.

As it was found out in previous simulation [3], the perturbation terms δ_j have no influence on the blow-up, except that they can considerably increase the time when the blow-up sets in. The behavior of the solution near the critical time τ is remarkably stable with respect to the perturbation terms. Therefore in order to save computer time we assumed $\delta_j(k_1, k_2) = 0$, $j = 1, 2$.

Computations were also performed with initial data of the type (3.5), but with a function $\mathbf{H}$ which is not a fixed point, in particular with the function

$$\mathbf{H}_\alpha(k_1, k_2) = -2 \left(k_1 - \alpha k_2, k_2 + \alpha k_1 \right), \qquad \alpha \geq 1. \qquad (3.6)$$

This choice was made in view of the fact that the real flow obtained by antisymmetrizing the initial data (3.6) is axial symmetric with a swirl depending on α.

The main indication from our simulations for the complex case is that all the initial data described above lead to a blowup in a range of values of the parameters which are more or less the same in all cases. Also the divergence rates of the total energy and enstrophy seem to be the same. Therefore it appears that the blow-up is a more general feature than convergence to a fixed point, although it is unclear whether it is a general consequence of the choice of the initial support. We hope that it will be possible to get some rigorous result on this point.

We studied in particular the case with initial data given by (3.5), (3.6) with $\delta_j = 0$, which are not related to solutions of the fixed point equation. The simulations show that the blow up occurs in a way remarkably similar to that of the solutions related to the Li-Sinai case (2.23). As in that case, the marginal distributions of the energy and the enstrophy along the k_3-axis, i.e.,

$$
\begin{aligned}
E_3(k_3) &= \tfrac{1}{2} \int_{\mathbb{R}^2} |\mathbf{v}(k_1, k_2, k_3, t)|^2 dk_1 dk_2, \\
S_3(k_3) &= \int_{\mathbb{R}^2} |\mathbf{k}|^2 |\mathbf{v}(k_1, k_2, k_3, t)|^2 dk_1 dk_2
\end{aligned}
\tag{3.7}
$$

show that the support is concentrated around the planes $k_3 \approx pa$, for $p = 1, 2, \ldots$ (Fig. 1).

Moreover, as we approach the blow-up, the fall-off for large p of the contributions to $E_3(k_3)$ at $k_3 \approx pa$ looks exponential with a coefficient that near the blow-up is proportional to $\tau - t$ (Fig. 2), where the critical time τ is estimated by the intersection of the linear plot of $\log E_3(k_3)$ with the horizontal axis (Fig. 3). For the function S_3 there is a power law correction $\mathcal{O}(p^2)$, which spoils linearity near the critical time.
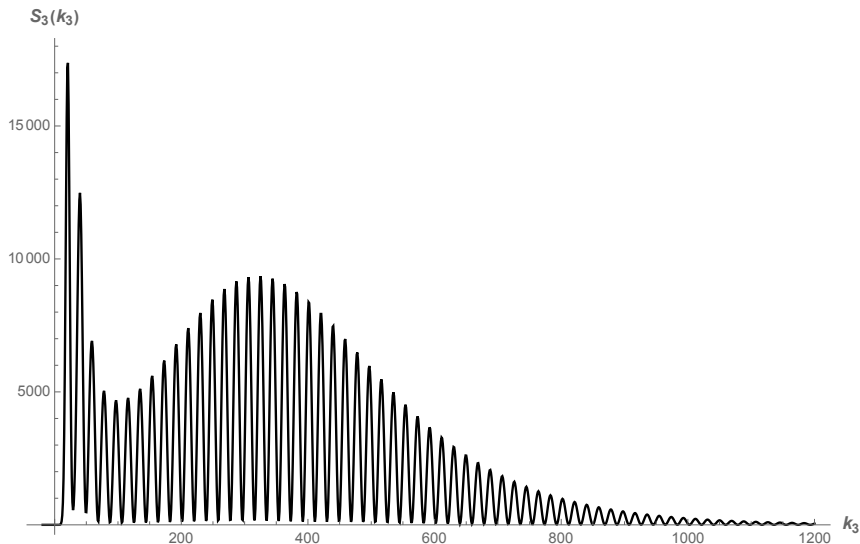
Figure 1: Plot of the marginal enstrophy density $S_3(k_3, t)$ at the time $t \times 10^7 = 2850$.
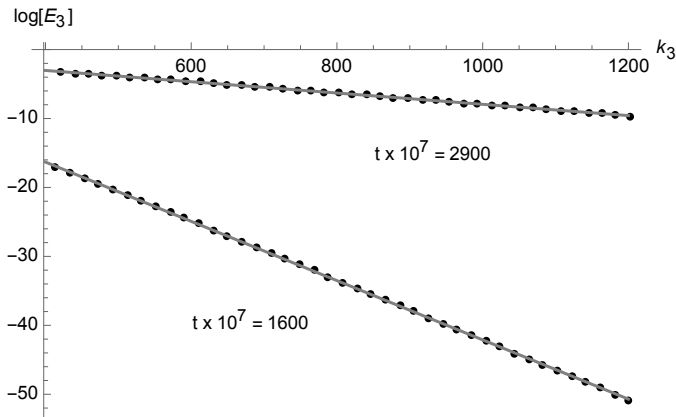
Figure 2: Plots of the peak values of $\log E_3(k_3, t)$ at two different times.
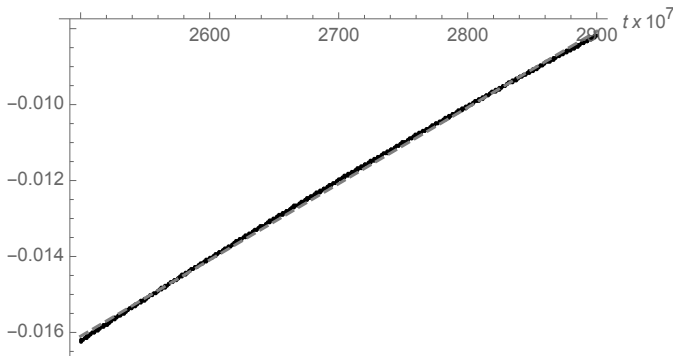
Figure 3: Plot of the slope (peak values) of $\log E_3(k_3, t)$ in time.

The results suggest that the contributions for $k_3 \approx pa$ have, for large p, as in the *Ansatz* (2.20) for the Li-Sinai case, a factor of the type $(\frac{\Lambda(t)}{\Lambda(\tau)})^p$, $t < \tau$, where $\Lambda(t)$ is an increasing differentiable function. If this happens, the exponential rate of decay near the blow-up time is related to the derivative $\Lambda'(\tau)$ by the Taylor formula

$$\log \left[\frac{\Lambda(t)}{\Lambda(\tau)} \right]^p = p \left[\log 1 - (\tau - t) \frac{\Lambda'(\tau)}{\Lambda(\tau)} (1 + o(1)) \right] \approx -p \frac{\Lambda'(\tau)}{\Lambda(\tau)} (\tau - t).$$
(3.8)

The power laws of the blow-up for the total energy $E(t) \asymp C_E (\tau - t)^{-\frac{1}{2}}$ and the total enstrophy $S(t) \asymp C_E (\tau - t)^{-\frac{5}{2}}$ predicted for the Li-Sinai case,

seem to hold in this case as well (Fig. 4)
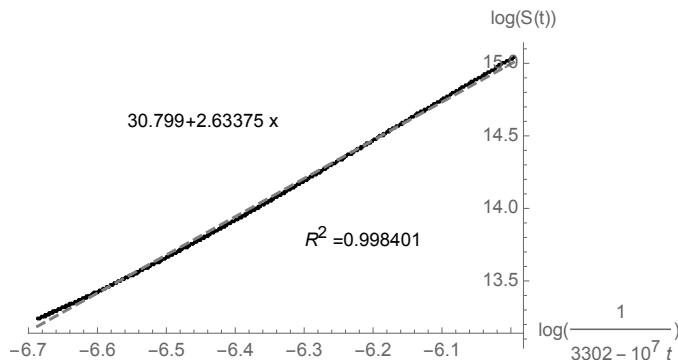
Figure 4: Plot of $\log S(t)$ versus $\log(\frac{1}{3302-10^7 t})$.

The main difference with the Li-Sinai case is however that there is no convergence to a fixed point for the vector field around the points $p\mathbf{k}^{(0)} = (0,0,pa)$ for large p. We have instead what looks like some kind of periodic behavior on the planes $k_3 \approx pa$, alternating situations in which the projection of the velocity field $\mathbf{v}(k_1,k_2,k_3)$ is essentially radial and situations with a large angular component.

The divergence rate of the total energy and enstrophy at the critical time are compatible with the corresponding values for the Li-Sinai case as reported in [5], i.e.. $E(t) \asymp C_E(\tau - t)^{-\frac{1}{2}}$ and $S(t) \asymp C_S(\tau - t)^{-\frac{5}{2}}$ (Fig. 4)

4   Computer simulations for an axial symmetric flow with swirl

In a previous paper [4] we reported results on a real flow with initial data obtained by antisymmetrizing the initial data (3.5) with the Li-Sinai fixed point (2.23). The flow is axial symmetric with no swirl if the correction $\delta_j, j = 1, 2$ in (3.5) is set equal to zero, and we know (see [11]) that a blow-up is excluded for flows close to axial symmetric flows with no swirl.

Nevertheless the computer simulations reported in [4] show that the real flows related to the Li-Sinai solution share with their complex counterpart some important features, such as a rapid extension of the support to high values of $|\mathbf{k}|$ by the convolution mechanism, and an exponential decay of the energy along the k_3-axis with a decay rate which decreases in time in absolute value. The total enstrophy undergoes a rapid increase: for the choice of the initial energy and of the parameter a in [4] it grows by a factor

2. The maximal value of the velocity in physical space $\max_{\mathbf{x} \in \mathbb{R}^3} |\mathbf{u}(\mathbf{x}, t)|$ also grows, and there is a remarkable concentration of energy and vorticity in a small volume. After some time however the exponential decay rate stops at some nonzero value and relaxation occurs with a decrease of the total enstrophy.

In our recent simulations we considered initial data with swirl related to solutions of the fixed point equation, and also initial data obtained by antisymmetrizing the expression (3.5) where $\mathbf{H} = \mathbf{H}_\alpha$ is given by (3.6), with $a = 20$, for which, as we showed above, there is a complex blow-up similar to that obtained with Li-Sinai initial data (2.23), although it is not related to a solution of the fixed point equation. We only report results for the latter case which, up to now, looks more promising for the Global Regularity Problem.

Neglecting the perturbation $\delta_j, j = 1, 2$, and a positive factor which fixes the initial energy, the initial data are

$$\mathbf{v}_0(k_1, k_2, k_3) = \left(k_1 - \alpha k_2, k_2 + \alpha k_1, -\frac{k_1^2 + k_2^2}{k_3} \right) \cdot$$

$$\cdot g_\sigma(k_1) g_\sigma(k_2) \left[g_\sigma(k_3 - a) \chi_b(k_3 - a) + g_\sigma(k_3 + a) \chi_b(k_3 + a) \right]. \quad (4.1)$$

The vector field (4.1) differs from the corresponding initial data related to the Li-Sinai solution only for an angular component proportional to α. It is easy to see that the initial condition in the physical $\mathbf{x}$-space, obtained by the inverse formula (2.6), is axial symmetric with a nonzero swirl proportional to α. As a consequence, the solution $\mathbf{u}(\mathbf{x}, t), t \geq 0$ following from the initial data (4.1) is also axial symmetric with nonzero swirl.

We performed simulations with the initial data (4.1) for $a = 20$, $\alpha = 1, 2, 5$, and for various values of the initial energy. We obtained a large amount of data which are still under study. The simulations show that by adding a swirl the growth of the enstrophy is greatly increased, and other interesting features also appear. We report here the first most relevant results concerning the initial data (4.1) with $\alpha = 2$, which produces the largest relative growth of the total enstrophy.

The mesh for the computer simulations is as in the previous section, except that it was doubled by adding the symmetric mesh in the half-space $k_3 \leq 0$. Significant results are obtained for a time step smaller than in the complex case and much higher initial energies. The time unit is $\delta_t = 1.562 \times 10^{-8}$.

The simulations show (Fig. 5) that we have, as for the complex case, a significant extension of the support along the k_3-axis, which causes the increase of the total enstrophy, while the energy goes down.
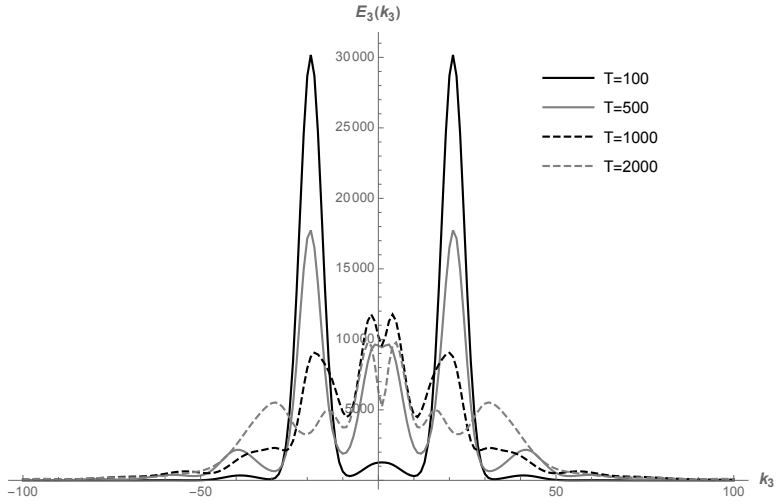
Figure 5:   Results for the initial data (4.1) with $\alpha = 2$. Initial energy $E_0 = 500000$. Time T is in units $\delta_t = 1.562 \times 10^{-8}$. Plot of the marginal energy density $E_3(k_3, t)$ at different times.
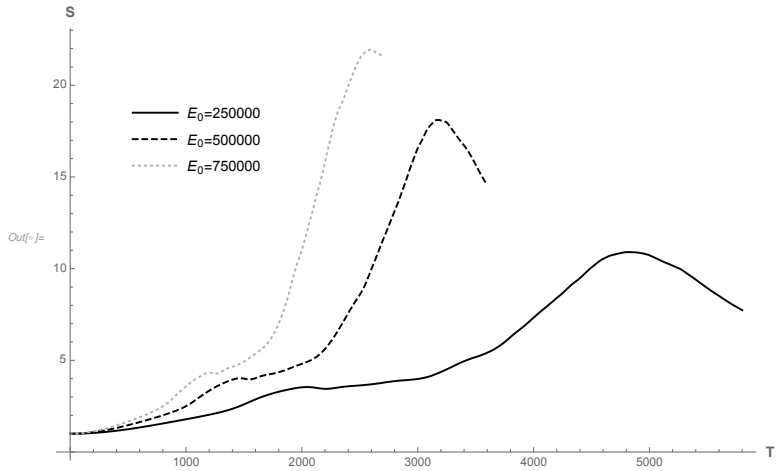
Figure 6:   Results for the initial data (4.1) with $\alpha = 2$. Time T is in units $\delta_t = 1.562 \times 10^{-8}$. Plots of the total enstrophy ratio $S(t)/S(0)$ for three values of the initial energy.

In Fig. 6 we report the relative growth of the total enstrophy for $\alpha = 2$ and different values of the initial energy E_0. It is much higher than for the case $\alpha = 0$ reported in [4] with equal initial energy $E_0 = 250 \times 10^3$, and the growth with the initial energy is also considerable. This result has to be taken with some caution, as we still need to estimate the contribution of the spurious production of enstrophy on the boundary, but we do not expect that it will produce a qualitative change of the picture.

The occurrence of a finite-time blowup for higher values of the initial energy and/or of the parameter a cannot be excluded, and it seems possible to obtain a better picture with more computer resources.

The results obtained from the simulations of the real flows are still under study. We will analyze in particular the evolution of the distribution in space and time of the local energy and rotation, for a comparison with the recent theoretical results on the regularity of the Navier-Stokes solutions as discussed in [1], [2], [7], [8], [16].

5   Concluding remarks

We report some preliminary results of computer simulations of the incompressible Navier-Stokes equations in 3D in Fourier **k** space, in absence of boundary conditions and forcing, with support of the type introduced by Li and Sinai [13]. Although the full analysis of the results is still under way, we can already draw some important indications.

For the complex solutions, the results show that a blow-up of the type described in the rigorous results of Li and Sinai [13] occurs, with similar features, for a wide class of initial data, both related and unrelated to the solutions of the fixed point equation (2.21).

We also present results of real flows obtained from complex flows that blow up by antisymmetrizing the initial data. The simulations show that for axial symmetric initial data the presence of a swirl of size comparable to that of the radial component produces a much larger increase of the total enstrophy for the same initial energy. Moreover the relative increase of the enstrophy grows as we increase the initial energy in a significant way.

The data from the simulations are however insufficient for a reasonable statement on the possibility of obtaining a blow-up by increasing the initial energy or the distance a of the support center from the origin. It is however reasonable to guess that more simulations could shed some light on this point.

References

[1] H. Beirao da Veiga. Viscous incompressible flows under stress-free boundary conditions. The smoothness effect of near orthogonality and near parallelism between velocity and vorticity. *Bollettino B.U.M.I.*, V:225–232, 2012.

[2] H. Beirao da Veiga and L. C. Berselli. Navier-Stokes equations: Green's matrices, vorticity direction and regularity up to the boundary. *J. Diff. Equations*, 246:597–628, 2009.

[3] C. Boldrighini, S. Frigio, and P. Maponi. On the blow-up of some complex solutions of the 3D Navier-Stokes Equations: theoretical predictions and computer simulation. *IMA J. Math. Phys.*, 83:697–714, 2017.

[4] C. Boldrighini, S. Frigio, P. Maponi, A. Pellegrinotti, and Ya. G. Sinai. Antisymmetric Solution of the 3D Incompressible Navier-Stokes Equations with "Tornado-like" Behavior. *J. Exp. Theor. Phys.*, 131:356–360, 2020.

[5] C. Boldrighini, D. Li, and Ya. G. Sinai. Complex singular solutions of the 3-d Navier-Stokes equations and related real solutions. *J. Stat. Phys.*, 167(1):1–13, 2017.

[6] A. Cheskidov. Blow-up in finite time for the dyadic model of the Navier-Stokes equations. *Trans. Am. Math. Soc.*, 360(10):5101–5120, 2008.

[7] P. Constantin and C. Fefferman. Direction of vorticity and the problem of global regularity of the Navier-Stokes equations. *Indiana Univ. Math. J.*, 42:775–789, 1993.

[8] A. Farhat and Z. Grujic. Local Near-Beltrami Structure and Depletion of the Nonlinearity in the 3D Navier-Stokes Flows. *J. Nonlinear Sci.*, 29(2):823–838, 2019.

[9] Th. Y. Hou. Blow-up or no blow-up? A unified computational and analytic approach to three-dimensional incompressible Euler and Navier-Stokes equations. *Acta Numer.*, 18:277–346, 2008.

[10] N. Katz and N. Pavlovic. Finite time blow-up for a dyadic model of the Euler equations. *Trans. Am. Math. Soc.*, 357(2):695–708, 2004.

[11] Z. Lei and Q. Zang. Criticality of the axially symmetric Navier-Stokes equations. *Pac. J. Math.*, 289:169–187, 2017.

[12] J. Leray. Sur le mouvement d'un liquide visqueux emplissant l'espace. *Acta Math.*, 63:193–248, 1934.

[13] D. Li and Ya. G. Sinai. Blowups of complex solutions of the 3D Navier-Stokes system and renormalization group method. *J. Eur. Math. Soc.*, 10:267–313, 2008.

[14] D. Li and Ya. G. Sinai. Blowups of Complex-valued Solutions for Some Hydrodynamic models. *Regul. Chaotic Dyn.*, 15(4-5):521–531, 2010.

[15] D. Li and Ya. G. Sinai. Singularities of complex-valued solutions of the two-dimensional Burgers system. *J. Math. Phys.*, 51:015205, 2010.

[16] A. Ruzmaikina and Z. Grujic. On Depletion of the Vortex-Stretching Term in the 3D Navier-Stokes Equations. *Commun. Math. Phys.*, 247:601–611, 2004.

[17] G. Seregin. A Certain Necessary Condition of Potential Blow up for Navier-Stokes Equations. *Commun. Math. Phys.*, 312:833–845, 2012.

[18] T. Tao. Finite time blowup for an averaged three-dimensional Navier-Stokes equation. *J. Amer. Math. Soc.*, 29(3):601–674, 2016.

[19] R. Temam. *Navier-Stokes Equations.* North Holland, 1979.

C. Boldrighini
Istituto Nazionale di Alta Matematica
Università di Roma Tre
Largo S. Leonardo Murialdo 1
00146 Rome, Italy

S. Frigio
Scuola di Scienze e Tecnologie
Università di Camerino
62932 Camerino, Italy

P. Maponi
Scuola di Scienze e Tecnologie
Università di Camerino
62932 Camerino, Italy

A. Pellegrinotti ✉
Dipartimento di Matematica e Fisica
Istituto Nazionale di Alta Matematica
Università di Roma Tre
00146 Rome, Italy
pellegri@mat.uniroma3.it

Ya. G. Sinai
Dept. of Mathematics,
Princeton University and
Russian Academy of Sciences